2008 IEEE International Conference on
Robotics and Automation
Pasadena, CA, USA, May 19-23, 2008

# GPS Denied Source Seeking For Underactuated Autonomous Vehicles in 3D

Jennie Cochran, Antranik Siranosian, Nima Ghods and Miroslav Krstic

*Abstract*— **Extremum seeking has been successfully applied to source seeking for autonomous vehicles operating in two dimensions. In this paper we extend these results to vehicles operating in three dimensions. The extension is interesting for several reasons. First, there is the choice of vehicle models to consider, and second there is the question of what type of vehicle movement can be actuated. We present two control schemes which address these questions. The first scheme focuses on vehicles with a constant forward velocity and the ability to actuate pitch and yaw velocities. The second scheme explores vehicles which operate with a constant forward velocity and a constant pitch velocity and which are capable of actuating only the roll velocity. We present the vehicle models, details of the control schemes, and simulation results.**

## I. Introduction

The field of study for autonomous vehicles operating without GPS or inertial navigation is an area of rapidly growing interest. In environments where GPS is unavailable and inertial navigation is too costly, such as urban, underground and underwater environments, other methods must be employed to navigate vehicles. Extremum seeking applied to source seeking has been presented as a method for autonomous vehicles to locate a target which emits some sort of measurable signal [1], [2]. This signal could be electromagnetic, acoustic or the concentration of a chemical or biological agent. The extremum seeking method uses only the measurement of the signal from the vehicle's sensor and then employs a periodic probing movement for the vehicle to navigate the field and locate the target. Results of applying this method to vehicles operating in two dimensions show its great potential for use in many applications [3]. In this paper we explore the use of extremum seeking for the navigation of vehicles operating in three dimensions. The extension to three dimensions is interesting for several reasons. First, there is the choice of vehicle models to consider and secondly there is the question of what type of vehicle movement can be actuated. We choose a model which is easily applied to several different types of vehicles, and we explore different types of actuation for these vehicles.

While other groups have considered source seeking problems, [4] and [5], this work is different in that the vehicle has no knowledge of its position or the position of the source, there is no communication between it and other entities, and it has nonholonomic dynamics. While we apply the extremum seeking methods to autonomous vehicles, many groups have used the extremum seeking method in their work outside of this field, including [6], [7], [8], [9], [10], [11], [12], [13], [14] and [15].

We present two control schemes for actuating an autonomous vehicle operating in three dimensions, to locate a target which emits some signal the vehicle can sense. The first scheme addresses vehicles which have a constant forward velocity and can actuate both yaw and pitch velocities. We refer to this vehicle as the VYPa (Vehicle Yaw and Pitch actuated). The second scheme addresses vehicles which also have a constant forward velocity as well as a constant pitch velocity, but can only actuate the roll velocity. We refer to this vehicle as the VeRa (Vehicle Roll actuated).

This paper starts with an overview of the extremum seeking method applied to source seeking in section II and then continues with section III, in which the vehicle model is discussed. Sections IV and V detail the VYPa and VeRa control schemes respectively. Within each of these two sections, we discuss the specific control scheme and present simulation results. We continue with section VI where we present the application of the method to level set tracing. Section VII concludes the paper with our intentions for future work.

## II. Overview of Extremum Seeking for Autonomous Vehicles

Extremum seeking employs periodic forcing of a plant (in this case an autonomous vehicle) to perform non-model based gradient estimation [16]. The vehicles considered are kinematically constrained, must navigate to perform some task, and have no position information available. Considering these constraints, one of the methods successes is simultaneously solving a non-holonomic steering problem and an adaptive optimization problem.

The extremum seeking method applied to source seeking works under the assumption that a target creates some signal field that a vehicle can sense at a distance away from the target. The shape of the signal field is unknown, though the strength of the signal is assumed to be a maximum at the target and to decay with distance away from it. This assumption is valid for many types of signal fields such as electromagnetic fields, acoustic fields, dissipative chemical or biological fields, and light/luminous fields. A vehicle employing extremum seeking uses only the scalar measure of the signal field at the position of its sensor (at the tip of the vehicle) as an input to the control loop. The vehicle employs periodic probing to search its surroundings and a bias term to turn in the correct direction. This combination

This work was supported by NSF and an NDSEG Fellowship.

J. Cochran, A. Siranosian, N. Ghods and M. Krstic are with Department of Mech. and Aero. Engineering, University of California, San Diego, 9500 Gilman Dr., La Jolla, CA 92093, USA jcochran@ucsd.edu

allows it to perform gradient estimation and converge to the vicinity of the target. As stated, all of this is achieved without the use of positioning information such as GPS or inertial navigation, and without the use of communication with other entities. If position information were available and the shape of the signal field were known, then we could easily design a control law to force the vehicle's trajectory to evolve according to the gradient dynamical system $\dot{r}_c = -\nabla f$ where $f$ represents the signal field. This law would allow the vehicle to asymptotically converge to an extremum of the signal field. But without this knowledge, we resort to other methods, such as techniques of non-model based optimization. Therefore in urban, underground and underwater environments, where GPS is unavailable, and in applications where inertial navigation is too expensive to implement, extremum seeking proves to be extremely useful.

Previous work has employed extremum seeking for vehicles operating in two dimensions, modeled as a non-holonomic unicycle

$$\dot{r}_c = v e^{j\theta} \quad (1)$$
$$\dot{\theta} = \Omega \quad (2)$$

where $r_c$ is the vector position of the vehicle center, $\theta$ is the vehicle orientation and $v$ and $\Omega$ are the forward and angular velocity inputs [2], [3]. These vehicles are given a constant forward velocity, $v = V_c$, while the angular velocity is tuned by extremum seeking ,

$$\Omega = a\omega\cos(\omega t) + c\sin(\omega t)\frac{s}{s+h}[J] \quad (3)$$

where $a, c, h$ and $\omega$ are parameters of the law and $J$ is the value of the signal reading $f$ from the vehicle sensor located at $r_s = r_c + Re^{j\theta}$. The first term, $a\cos(\omega t)$ is a continuous periodic (persistent) excitation of the angular velocity which allows the vehicle to fully probe the area and records differences in signal readings. The frequency $\omega$ must be relatively high for the scheme to work, while the amplitude $a$ is usually between 1/3 and unity. The second term is a bias which turns the vehicle in the correct direction. It accomplishes this by first sending the sensor reading $J$ through a washout filter $\frac{s}{s+h}[J]$ to eliminate the DC component and focus on the gradient signal. The filtered signal is then multiplied by $\sin(\omega t)$ to demodulate it from the probing signal - the first term. The gain $c$ is adjusted to make the vehicle's reaction to the signal field more or less aggressive. The result of applying this control law to the unicycle model is the exponential convergence of the vehicle to the vicinity of the signal source. We extend this model to three dimensions and show how extremum seeking is applied to two different cases, achieving the same goal as always, performing gradient estimation to locate the source of a signal.

## III. Vehicle Model

When extending the vehicle model from two dimensions to three, we had to consider how to accurately represent a kinematically constrained vehicle which could support different

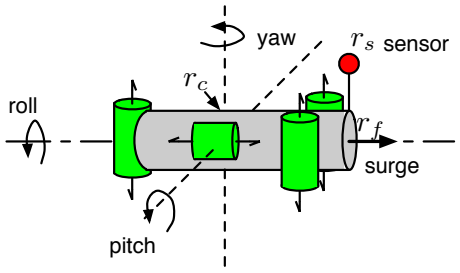


Fig. 1. Pictorial drawing of the 3D vehicle.

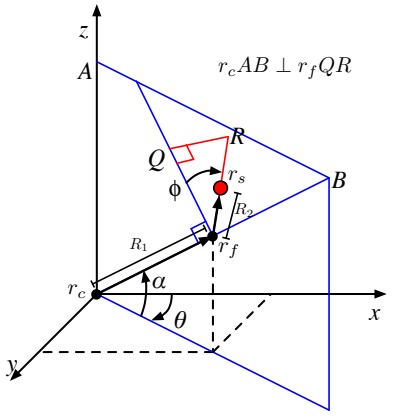


Fig. 2. Graphical interpretation of vehicle in 3D.

vehicle configurations. We chose a kinematic model, depicted in Figure 1, which shows a vehicle whose actuators, shown as cylinders with half arrows, can be used to impart surge, yaw, pitch and roll velocities. The center of the vehicle is labeled $r_c$, the front of the vehicle is labeled $r_f$. The sensor, shown as a sphere, is located above $r_f$ at $r_s$. Figure 2 contains a geometric interpretation of the drawing in Figure 1. In the coordinate system shown, $R_1$ is the distance between the center $r_c$ and the front $r_f$, while $R_2$ is the distance between the front $r_f$ and the sensor $r_s$. The vector between $r_f$ and $r_s$ is always perpendicular to the vector between $r_c$ and $r_f$. The pitch of the vehicle is defined by $\alpha$, the azimuthal angle. The yaw of the vehicle is defined by $\theta$, the polar angle. The third possible vehicle rotation, roll, is defined by $\phi$, and is measured in the plane containing $r_fQR$ relative to the plane containing $r_cAB$. The surge velocity, $v_1$, acts in the direction of $\overline{r_c r_f}$ while the pitch velocity $v_2$ acts in the direction of $\overline{r_f r_s}$. The azimuthal velocity $\dot{\alpha}$ and polar velocity $\dot{\theta}$, or roll velocity $\dot{\phi}$ are available as control inputs.

The equations that govern the center of the vehicle model depicted in Fig. 2 are

$$\dot{x}_c = v_1\cos(\alpha)\cos(\theta) \quad (4)$$
$$\dot{y}_c = v_1\cos(\alpha)\sin(\theta) \quad (5)$$
$$\dot{z}_c = v_1\sin(\alpha) \quad (6)$$
$$(7)$$

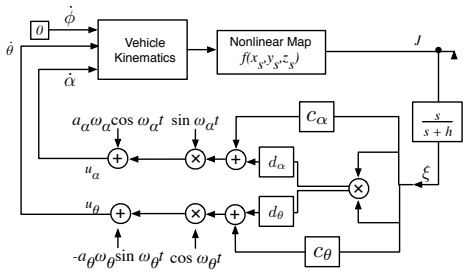


Fig. 3. Block diagram of ES control applied to the pitch and yaw velocities of the VYPa.

where $r_c = (x_c, y_c, z_c)$. The sensor position is

$$\begin{aligned} x_s &= x_c + R_1\cos\alpha\cos\theta \\ &\quad + R_2\left(-\cos\phi\sin\alpha\cos\theta + \sin\phi\sin\theta\right) \quad (8) \\ y_s &= y_c + R_1\cos\alpha\sin\theta \\ &\quad + R_2\left(-\cos\phi\sin\alpha\sin\theta - \sin\phi\cos\theta\right) \quad (9) \\ z_s &= z_c + R_1\sin\alpha + R_2\cos\phi\cos\alpha\,, \quad (10) \end{aligned}$$

where $r_s = (x_s, y_s, z_s)$.

This model is used for both control schemes presented. The similarities and differences will be summarized here and expanded in the next sections. In both schemes, the surge velocity, $v_1$, is set to a non-zero constant. In the first scheme, applied to the VYPa, the sensor is placed at the tip of the vehicle, i.e., $R_2 = 0$, so the roll velocity and angle play no role. Extremum seeking is used to tune the remaining control inputs, the pitch and yaw velocities. In the second scheme, applied to the VeRA, the pitch velocity, $v_2$, is also set to a non-zero constant and extremum seeking only tunes the roll velocity for control. The distance between the tip of the vehicle and the sensor, $r_s$ must be nonzero in this case.

## IV. VYPa Vehicles

The first scheme we address is tuning for the Vehicle Yaw and Pitch actuated – VYPa. This vehicle has a constant forward velocity, $v_1$, a constant roll angle of zero, and, as the name indicates, is capable of actuating its pitch and yaw velocities. The sensor is located at the tip of the vehicle, which equates to setting $R_2 = 0$. Its position with respect to the vehicle center reduces to

$$\begin{aligned} x_s &= x_c + R_1\cos\alpha\cos\theta \quad (11) \\ y_s &= y_c + R_1\cos\alpha\sin\theta \quad (12) \\ z_s &= z_c + R_1\sin\alpha\,. \quad (13) \end{aligned}$$

As the surge velocity is constrained to one axis in the body frame and the angular velocity is always around an axis orthogonal to that of the surge velocity, this the 3D analog of the unicycle.

Figure 3 shows a block diagram of the control applied to the VYPa, with extremum seeking used to tune the pitch and yaw velocities. When the roll angle is kept at zero, tuning the pitch velocity is equivalent to tuning $\dot{\alpha}$, and tuning the yaw velocity is equivalent to tuning $\dot{\theta}$. The designer is free to choose the perturbation amplitudes $a_\alpha$, $a_\theta$, the perturbation frequencies $\omega_\alpha$, $\omega_\theta$, the extremum seeking gains $c_\alpha$, $c_\theta$, and the break frequency $h$ of the filter. It should be noted that, by construction, $\omega_\theta$ can be the same as $\omega_\alpha$. The perturbation amplitude affects the how steep the gradient must be for the vehicle to be able to discern a nonzero gradient. The higher the perturbation frequencies the more accurate the gradient estimation becomes. The extremum seeking gains affect the aggressiveness of the control. The VYPa model dynamics remain (4)–(6), while the control inputs, following from Figure 3, are

$$\begin{aligned} \dot{\alpha} &= a_\alpha\omega_\alpha\cos(\omega_\alpha t) + c_\alpha\sin(\omega_\alpha t)\,\frac{s}{s+h}\,[J] \quad (14) \\ \dot{\theta} &= -a_\theta\omega_\theta\sin(\omega_\theta t) + c_\theta\cos(\omega_\theta t)\,\frac{s}{s+h}\,[J] \quad (15) \\ \dot{\phi} &= 0 \quad (16) \end{aligned}$$

where $\frac{s}{s+h}[J]$ is a washout filter applied to the sensor reading $J$.

As usual, the extremum seeking tuning consists of both 1) periodic perturbations, $a_\alpha\omega_\alpha\cos(\omega_\alpha t)$ and $-a_\theta\omega_\theta\sin(\omega_\theta t)$, which allow for searching the signal field, and 2) bias terms, $c_\alpha\sin(\omega_\alpha t)\,\frac{s}{s+h}\,[J]$ and $c_\theta\cos(\omega_\theta t)\,\frac{s}{s+h}\,[J]$, which turn the vehicle in the correct direction. The bias terms are composed of the high-pass filtered demodulated sensor measurement, multiplied by the appropriate gains.

Figure 5 shows a VYPa vehicle tracking a source which remains in one position. Analysis of the 2D control scheme [2], [17] is done with a signal field of the form $J = f^* - q_x(x_s - x^*)^2 - q_y(y_s - y^*)^2$. The scheme presented here works for fields of this form and many other forms, such as the one we chose to use here

$$J = \frac{f_{max}}{1 + q_x(x_s - x^*)^2 + q_y(y_s - y^*)^2 + q_z(z_s - z^*)^2}\,,$$

where $(x^*, y^*, z^*) = r^*$ is the position of the source. The difference in the two maps can be seen in Figure 4 where graph (a) shows a 2D field used in analysis and (b) shows a 2D field of the type used in these simulations. Figure 5 shows the vehicle trajectory which heads toward the source and then settles on a trajectory which remains close to the source. It also shows the two dimensional projections of the trajectory in the $x-y$, $x-z$ and $y-z$ planes. The projection in $y-z$ shows a figure-eight trajectory, while the projections in $x-y$ and $x-z$ show banana like trajectories. Both the figure-eight and banana trajectories appear in the two dimensional extremum seeking results. Figure 6 shows the VYPa tracking a moving source/targert. The target moves as

$$\Big(x_t(t), y_t(t), z_t(t)\Big) = \Big(a_t\cos(\omega_t t), a_t\sin(\omega_t t), a_{tz}\sin(\omega_{tz} t)\Big).$$

The vehicle moves toward the source and then follows it around its path. Again, projections of the vehicle's trajectory are shown. Figure 7 shows the distance between the vehicle center $r_c$ and the source as they move around the region.

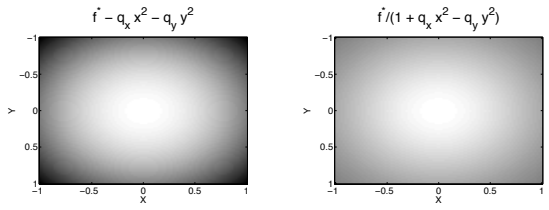


$(a)$ $(b)$

Fig. 4. Signal field. (a) Field used in 2D analysis. (b) 2D field of the type used in these 3D simulations. The parameters for both simulations are $f^* = 1, q_x = 0.5, q_y = 0.5$.

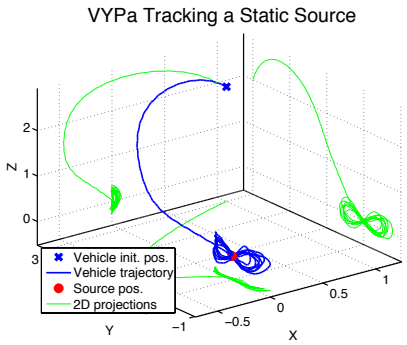


Fig. 5. VYPa tracking a static source. The trajectory of the vehicle center is shown. The figure-eight and banana trajectories appear in two dimensional simulation results as well. $f^* = 1, q_x = 1, q_y = 0.5, q_z = 0.75, r_1 = 0.1, v_1 = 0.09, a = 0.5, \omega = 10, c = 50, h = 1$

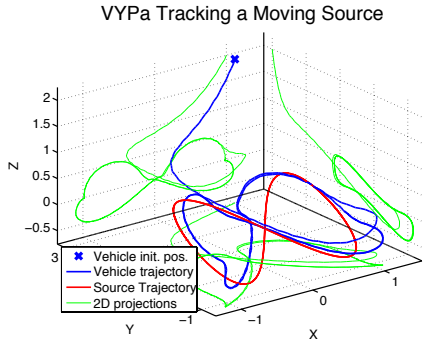


Fig. 6. VYPa tracking a moving source. The trajectory of the vehicle center is shown. $f^* = 1, q_x = 1, q_y = 0.5, q_z = 0.75, r_1 = 0.1, v_1 = 0.11, a = 0.5, \omega = 10, c = 50, h = 1, a_t = 1, a_{tz} = 0.5, \omega_t = 0.05, \omega_{tz} = 0.1$

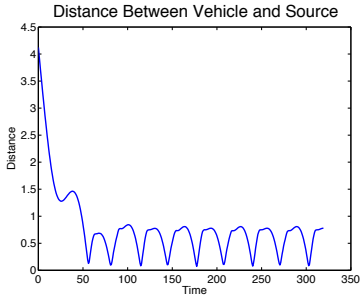


Fig. 7. Distance between the center of the VYPa vehicle and the moving source.

Initially this distance is large as the vehicle has yet to find the source, but once the vehicle gets close to the source, it remains close.

As mentioned the vehicle behavior seen with this control scheme is very similar to the behavior seen with the 2D vehicle. In particular, the same methods can be used to prove convergence of the scheme. Using averaging theory, it can be proved that if $\omega$ is large enough and the level sets of the signal field are spherical, then the control law

$$\dot{\alpha} = a_\alpha \omega_\alpha \cos(\omega_\alpha t) + \sin(\omega_\alpha t)\left(c_\alpha \xi - d_\alpha \xi^2\right) \quad (17)$$

$$\dot{\theta} = -a_\theta \omega_\theta \sin(\omega_\theta t) + \cos(\omega_\theta t)\left(c_\theta \xi - d_\theta \xi^2\right) \quad (18)$$

$$\xi = \frac{s}{s+h}[J] \quad (19)$$

produces locally exponentially convergence to the source. We do not use the extra term $d_i \xi^2$ in this paper, as simulations indicate that it is not needed for convergence when the level sets are not spherical or when the source is moving. In addition, analysis indicates that the extra term is needed not to approach the source, but to remain close once the source has been found.

## V. VeRa Vehicles

The second scheme presented is for the Vehicle Roll actuated –VeRa. We consider both vehicle configurations to show both the adaptability of extremum seeking, and its use for extremely underactuated vehicles. This vehicle has both a constant forward velocity, $v_1$, and a constant pitch velocity, $v_2$. The only tunable input, as the name indicates, is the roll velocity. In this case the sensor must be mounted off of the tip of the vehicle, which indicates $R_2 \neq 0$. The sensor must be mounted in this way so that the perturbation movement provides a full persistency of excitation and the vehicle can explore the entire signal field.

When the pitch velocity, $v_2$, is constant, the azimuthal and polar velocities become

$$\dot{\alpha} = \frac{v_2}{r_1}\cos\phi \quad (20)$$

$$\dot{\theta} = -\frac{v_2}{r_1}\frac{\sin\phi}{\cos\alpha}. \quad (21)$$

The VeRa model dynamics remain (4)–(6) with (20) and (21) governing $\dot{\alpha}$ and $\dot{\theta}$, and $\dot{\phi}$ is tuned by extremum seeking. The sensor coordinates also remain (8)–(10).

Figure 8 shows a block diagram of the control applied to the VeRa, with extremum seeking used to tune the roll velocity. The designer is free to choose the perturbation amplitude $a$, the perturbation frequency $\omega$, the extremum seeking gain $c$ and the break frequency $h$ while considering the same effects discussed in Section IV. The control input, following from Figure 8, is

$$u_\phi = a\omega\cos(\omega t) + c\sin(\omega t)\frac{s}{s+h}[J] \quad (22)$$

where again $\frac{s}{s+h}[J]$ is a washout filter applied to the sensor reading $J$. Similarly to the previous case, this control law is split into a periodic perturbation, $a\omega\cos(\omega t)$, and a bias term, $c\sin(\omega t)\frac{s}{s+h}[J]$.

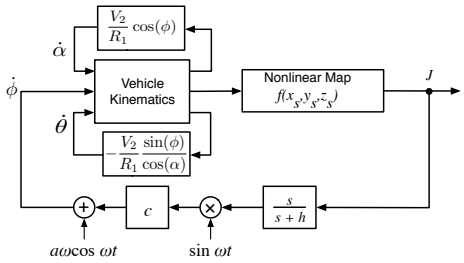


Fig. 8. Block diagram of ES control applied to the roll velocity of the VeRa.

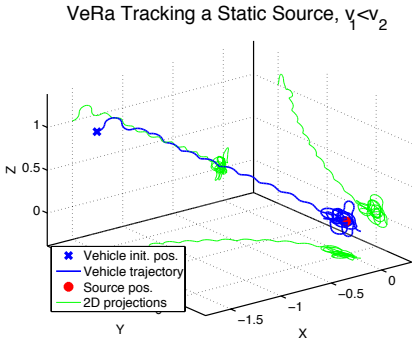


Fig. 9. VeRa tracking a static source. The tight curly trajectory of the vehicle center is a result of $v_1 < v_2$. $f^* = 1, q_x = 1, q_y = 1, q_z = 0.5, r_1 = 0.1, r_2 = 0.05, v_1 = 0.028, v_2 = 0.055, a = 1, \omega = 30, c = 400, h = 1$

Figures 9 and 12 show the VeRa locating a static source. An interesting difference between the simulations is the effect of the ratio of $v_1 : v_2$ on the behavior of the vehicle. This ratio dictates whether the VeRa makes tight curly turns, as in Figure 9 or wide sweeping turns as in Figure 12. This difference is seen again in Figures 10 and 13 where the VeRa is tracking a moving source. Figures 11 and 14 show the distance from the vehicle center $r_c$ to the source as time evolves.

## VI. Other Applications

The use of extremum seeking for navigation of vehicles in three dimension extends beyond source seeking. This method can also be used to explore the domain of the signal field. Other groups have looked at isoline/boundary/level set tracking [18]. However these methods require either multiple agents which must communicate, or require multiple sensors on a single agent. By employing a simple modification to the extremum seeking tuning, both the VYPa and VeRa can find and trace three dimensional level sets with only one sensor and without communication with other entities. This modification changes the input to the control laws from the sensor reading, $J$, to the quantity $-|J - J_d|$, where $J_d$ is the desired level set value. The absolute value operator is used to retain the shape of the original signal field, as opposed to another operator, such as a the square of the difference. The

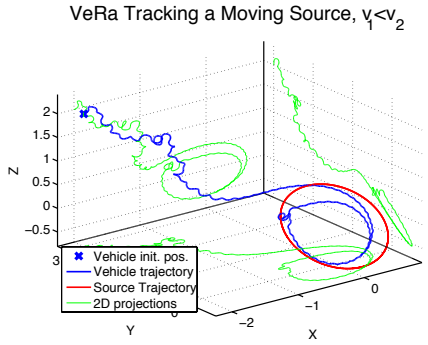


Fig. 10. Trajectory of the center of a VeRa vehicle tracking a moving source. $f^* = 1, q_x = 1, q_y = 0.5, q_z = 0.75, r_1 = 0.1, r_2 = 0.05, v_1 = 0.028, v_2 = 0.055, a = 1, \omega = 30, c = 400, h = 1, a_t = 0.7, a_{tz} = 0.6, \omega_t = 0.035, \omega_{tz} = 0.035$

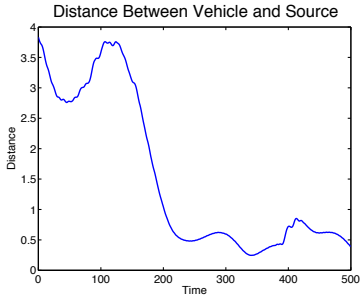


Fig. 11. Distance between the center of the VeRa vehicle and the moving source.

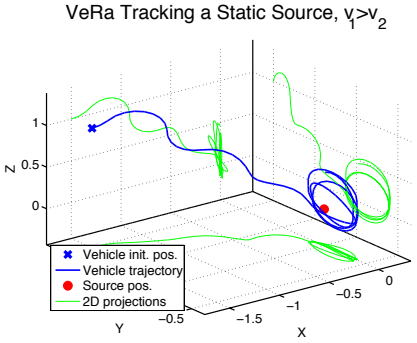


Fig. 12. VeRa tracking a static source. The wide turns of the vehicle center trajectory are a result of $v_1 > v_2$. $f^* = 1, q_x = 1, q_y = 0.5, q_z = 0.75, r_1 = 0.1, r_2 = 0.05, v_1 = 0.04, v_2 = 0.02, a = 1, \omega = 30, c = 400, h = 1$

control law in each case then becomes

$$u_i = a_i\omega_i\cos(\omega_i t) + c_i\sin(\omega_i t)\frac{s}{s+h}\left[-|J - J_d|\right] \quad (23)$$

Figures 15 and 16 show the differences in how the VYPa and VeRa trace out the same level set on the same signal field. Notice that the vehicles naturally move around the entire three dimensional space instead of repeatedly tracing out the same curve within the level set.

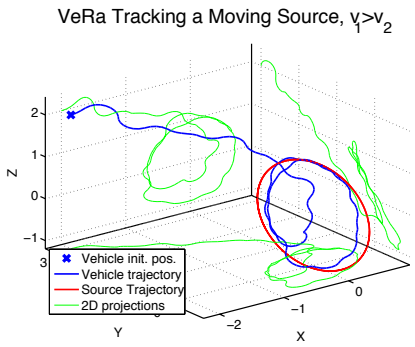


Fig. 13. Trajectory of the center of a VeRa vehicle tracking a moving source. $f^* = 1, q_x = 1, q_y = 0.5, q_z = 0.75, r_1 = 0.1, r_2 = 0.05, v_1 = 0.04, v_2 = 0.02, a = 1, \omega = 30, c = 400, h = 1, a_t = 0.75, a_{tz} = 1, \omega_t = 0.0385, \omega_{tz} = 0.0385$

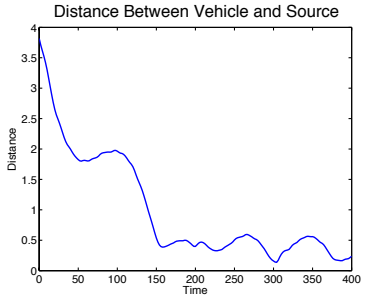


Fig. 14. Distance between the center of the VeRa vehicle and the moving source.

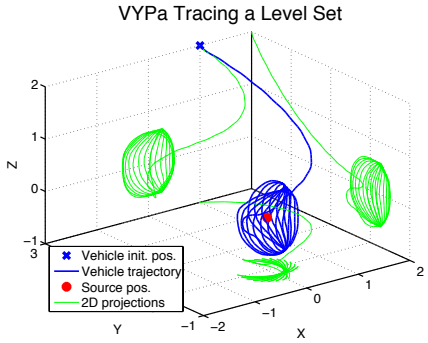


Fig. 15. VYPa tracing a levelset. The trajectory of the center of the vehicle is shown. $f^* = 1, q_x = 1, q_y = 1, q_z = 0.5, r_1 = 0.1, v_1 = 0.11, a = 0.5, \omega = 10, c = 50, h = 1, J_d = 0.8$

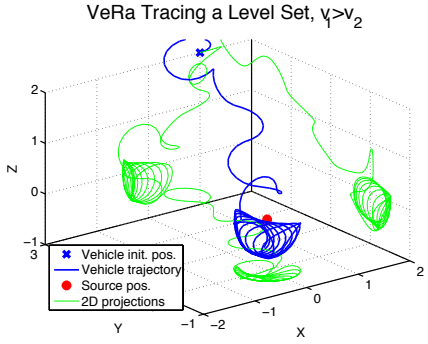


Fig. 16. VeRa tracing a levelset. The trajectory of the center of the vehicle is shown. $f^* = 1, q_x = 1, q_y = 1, q_z = 0.5, r_1 = 0.1, r_2 = 0.05, v_1 = 0.07, v_2 = 0.02, a = 0.75, \omega = 10, c = 500, h = 1, J_d = 0.8$

## VII. Conclusions and Future Work

We have shown how the extremum seeking method can be extended to vehicles with various actuating capabilities operating in three dimensions for carrying out tasks such as source seeking and boundary tracking. Future work includes producing source seeking stability results for the 3D vehicle models and exploring 3D boundary/levelset tracking for processes governed by diffusion and/or advection.

## References


[1] C. Zhang, D. Arnold, N. Ghods, A. Siranosian, and M. Krstic, "Source seeking with nonholonomic unicycle without position measurement and with tuning of forward velocity," *Systems and Control Letters*, vol. 56, pp. 245–252, 2007.

[2] J. Cochran and M. Krstic, "Source seeking with a nonholonomic unicycle without position measurements and with tuning of angular velocity — part I: Stability analysis," *2007 Conf. on Decision and Control*, 2007.

[3] J. Cochran, A. Siranosian, N. Ghods, and M. Krstic, "Source seeking with a nonholonomic unicycle without position measurements and with tuning of angular velocity — part II: Applications," *2007 Conf. on Decision and Control*, 2007.

[4] B. Porat and A. Neohorai, "Localizing vapor-emitting sources by moving sensors," *IEEE Trans. Signal Processing*, vol. 44, pp. 1018–1021, 1996.

[5] P. Ogren, E. Fiorelli, and N. Leonard, "Cooperative control of mobile sensor networks: adaptive gradient climbing in a distributed environment," *IEEE Trans. Automat. Contr.*, vol. 29, pp. 1292–1302, 2004.

[6] K. Peterson and A. Stefanopoulou, "Extremum seeking control for soft landing of and electromechanical valve actuator," *Automatica*, vol. 29, pp. 1063–1069, 2004.

[7] Y. Ou, C. Xu, E. Schuster, T. Luce, J. R. Ferron, and M. Walker, "Extremum-seeking finite-time optimal control of plasma current profile at the diii-d tokamak," *2007 American Ctrl. Conf.*, 2007.

[8] C. Centioli, F. Iannone, G. Mazza, M. Panella, L. Pangione, S. Podda, A. Tuccillo, V. Vitale, and L. Zaccarian, "Extremum seeking applied to the plasma control system of the Frascati Tokamak Upgrade," *44th IEEE Conf. on Decision and Ctrl., and the European Ctrl. Conf.*, 2005.

[9] Y. Tan, D. Nesic, and I. M. Y. Mareels, "On non-local stability properties of extremum seeking controllers," *Automatica*, vol. 42, pp. 889–903, 2006.

[10] R. King, R. Becker, G. Feuerbach, L. Henning, R. Petz, W. Nitsche, O. Lemke, and W. Neise, "Adaptive flow control using slope seeking," *14th IEEE Mediterranean Conf. on Ctrl. Automation*, 2006.

[11] R. Becker, R. King, R. Petz, and W. Nitsche, "Adaptive closed-loop separation control on a high-lift configuration using extremum seeking," *3rd AIAA Flow Control Conference*, 2006.

[12] M. Tanelli, A. Astolfi, and S. Savaresi, "Non-local extremum seeking control for active braking control systems," *Conference on Control Applications*, 2006.

[13] M. Guay, M. Perrier, and D. Dochain, "Adaptive extremum seeking control of nonisothermal continuous stirred reactors," *Chem. Eng. Science*, vol. 60, pp. 3671–3681, 2005.

[14] Y. Li, A. Rotea, G. T.-C. Chiu, L. Mongeau, and I.-S. Paek, "Extremum seeking control of a tunable thermoacoustic cooler," *IEEE Trans. Contr. Syst. Technol.*, vol. 13, pp. 527–536, 2005.

[15] X. Zhang, D. Dawson, W. Dixon, and B. Xian, "Extremum seeking nonlinear controllers for a human exercise machine," *Proc. 2004 IEEE Conf. Decision and Ctrl.*, 2004.

[16] K. Ariyur and M. Krstic, *Real-Time Optimization by Extremum-Seeking Control*. Hoboken, NJ: Wiley-Interscience, 2003.

[17] J. Cochran and M. Krstic, "Nonholonomic source seeking with tuning of angular velocity," *IEEE Trans. Automat. Contr.*, accepted with minor revision.

[18] S. Kalantar and U. Zimmer, "Control of open contour formations of autonomous underwater vehicles," *International Journal of Advanced Robotic Systems*, vol. 2, no. 4, pp. 309–316, Dec. 2005.